

Combining enhanced sampling with experiment-directed simulation of the GYG peptide

Dilnoza B. Amirkulova and Andrew D. White*

*Chemical Engineering
University of Rochester, Rochester
NY 14627, USA*

**andrew.white@rochester.edu*

Received 7 October 2017

Accepted 17 April 2018

Published 21 May 2018

Experiment-directed simulation (EDS) is a technique to minimally bias molecular dynamics simulations to match experimentally observed results. The method improves accuracy but does not address the sampling problem of molecular dynamics simulations of large systems. This work combines EDS with both the parallel-tempering or parallel-tempering well-tempered ensemble replica-exchange methods to enhance sampling. These methods are demonstrated on the GYG tripeptide in explicit water. The collective variables biased by EDS are chemical shifts, where the set-points are determined by NMR experiments. The results show that it is possible to enhance sampling with either parallel-tempering and parallel-tempering well-tempered ensemble in the EDS method. This combination of methods provides a novel approach for both accurately and exhaustively simulating biological systems.

Keywords: Molecular dynamic; experiment-directed simulation.

1. Introduction

Molecular simulations are connected to experiments through ensemble properties, called observables. Often, experimental and simulated values disagree due to challenges such as limited accuracy of force-fields and discrepancies between how experiments can be represented in a simulation. This disagreement can be improved by adding an auxiliary biasing potential energy function.^{1,2} For example, a simulation can be improved by incorporating experimental results as structural restraints in simulations.³ Often, these restraints are a type of harmonic energy penalty that brings conformational ensembles closer to the experimentally observed values.^{4,5} Visiting states that are outside structural restraints are unfavored with harmonic biases. This introduces some ambiguity in how strong these energetic restraints should be.

To address the ambiguity in using energetic restraints to match experimental data, a maximum entropy principle⁶ can be applied to find an energy bias that is

*Corresponding author.

minimal.^{7,8} This bias acts only in the dimension of the collective variable which corresponds to the experimental observable.⁹ Experiment-directed simulation (EDS) is an implementation of maximum entropy biasing. EDS uses an adaptive biasing method to converge to the maximum entropy bias that achieves agreement between molecular simulation collective variables and experimental observables.¹⁰ This bias is also provably the smallest change that can be made to match experimental data.^{8,10,11}

EDS utilizes a single replica, whereas most other maximum entropy methods utilize multiple replicas.¹ Other biasing methods, such as replica-exchange chemical shift restrained molecular dynamics simulations⁴ and restrained-ensemble molecular dynamics simulation method¹² that utilize multiple replicas require multiple replicas in order to match simulated results to some reference values. This increases the required computational effort, although there is an improvement in sampling due to the inherent increase of samples with the replicas. EDS, being a single-replica technique, provides no improvement to sampling. EDS has been applied to classical molecular dynamics,¹⁰ *ab initio* molecular dynamics¹³ and coarse-graining.¹⁴ EDS was able to give more accurate results on dynamic properties such as the self-diffusion coefficient of lithium in electrolyte solutions,¹⁰ and the proton-diffusivity in *ab initio* water¹³ as well.

EDS is a biasing method and this is designed to match the ensemble average of some collective variables to a certain reference value. EDS lets the underlying simulation determine the fluctuations and underlying distribution of the collective variable. Only the expected value is shifted to match the experimental value. Because EDS is only a method of simulation, it cannot correct or mitigate any error in the reference value, such as experimental error, human error, or instrumentation error. If the experimental value instead is a distribution or becomes a distribution, because a Bayesian inference approach with prior belief is desired, other techniques allow matching to that desired distribution like experiment-directed metadynamics¹¹ or metainference.¹⁵

Aside from accuracy, another challenge in molecular dynamics simulations is insufficient sampling of phase space. The so-called “sampling problem”¹⁶ is especially true in solvated macromolecules, where systems can become trapped in energy minima. EDS introduces a bias in the potential to match experimental averages; it is not an enhanced sampling technique. Thus, there is a need to use an enhanced sampling technique with EDS. Multiple enhanced sampling methods have been developed to alleviate this problem,¹⁷ often by biasing sampling to occur along a certain collective variable.¹⁸ This presents a complication with EDS if both enhanced sampling technique and EDS are applied on the same set of collective variables. For example, metadynamics¹⁹ will add Gaussian bias to the potential energy with respect to a collective variable, thereby modifying the potential of mean force (PMF) of that CV. EDS cannot be applied to a collective variable with a biased PMF because EDS requires canonical samples. For example, if metadynamics is applied to Φ dihedral angle and EDS is applied to Ψ dihedral angle, the Ψ angle needs to be re-weighted to

achieve canonical sampling due to bias on Φ and the inherent correlation between the Φ and Ψ . EDS needs the Ψ variable to be canonically sampled. Hence, EDS and Metadynamics cannot be applied simultaneously in a simulation. The well-tempered ensemble method (WTE) provides an alternative approach because it biases the fluctuations in energy, and with an assumption of the underlying potential energy distribution, does not affect the canonical sampling of other CVs. WTE can be further combined with parallel-tempering replica-exchange to improve the sampling further.^{20–22}

In this work, we consider the parallel-tempering well-tempered ensemble (PT-WTE) combined with EDS²² to improve both sampling and accuracy on an example system. Like in parallel-tempering replica-exchange, N replicas of the simulation system are run concurrently. The coldest replica is the system of interest, yet it can escape free energy minima by swapping configurations with higher temperatures. The goal of PT-WTE is to reduce the number of replicas while maintaining similar replica efficiency.²² It has been shown that PT-WTE metadynamics decreases the number of replicas from 100 to 10 while maintaining the similar energy landscape of solvated tryptophan-cage protein.²³ It has also been shown to improve speed of convergence to an accurate FES in model and real systems.^{22,23} The technique can be applied to larger systems such as proteins to efficiently sample their large conformational space.²⁴ The tri-peptide glycine–tyrosine–glycine (GYG) was used as a model system to demonstrate the implementation. GYG is found in structural and transport proteins, such as collagen²⁵ and ion channels.²⁶ Either mutations or complete deletions of this sequence from proteins showed complete or partial loss of a function in those proteins,^{27–29} so it has specific functional relevance. The experimental data utilized here are from backbone chemical shifts³⁰ of GYG peptide. These are used to assess accuracy of the simulation and the free energy surface along the Φ – Ψ dihedral angles is used to assess sampling.

Metadynamics metainference³¹ and replica-averaged metadynamics³² are the nearest examples of the method proposed here in the literature. Metadynamics metainference is a combination of the enhanced sampling technique of metadynamics¹⁹ with the ability to match the experimental data of metainference.³¹ Replica-averaged metadynamics is the combination of the replica-averaging approach to matching experimental data³² with the enhanced sampling of metadynamics. A distinguishing difference between our approach and these is that the biasing force from EDS can be calculated with an enhanced-sampling method first and then be applied to a second simulation without replicas. This capability allows dynamic properties like autocorrelation functions or diffusivities to be computed.

2. Theory

In the WTE method,²² Newton's equation of motion becomes

$$m\ddot{\mathbf{R}} = -\frac{U(\mathbf{R})}{\partial \mathbf{R}} - \frac{\partial V(U(\mathbf{R}), t)}{\partial \mathbf{R}}, \quad (1)$$

where m is the mass vector, \mathbf{R} is the position vector, $U(\mathbf{R})$ is the system potential energy and $V(\cdot)$ is a *time-dependent* function of the instantaneous potential energy which biases the system. $V(\cdot)$ is defined with the following time-derivative:

$$\dot{V}(U, t) = \omega e^{-V(U, t)/k_B \Delta T} \delta(U - U(t)), \quad (2)$$

where ω and ΔT are tuned constants. The intuition of this equation is to add a Gaussian at each time t centered at $U(t)$, just like in the metadynamics method.^{19,33} The key parameter in WTE is the bias factor, like in well-tempered metadynamics,³³ which is defined relative to system temperature and ΔT as $\gamma = (T + \Delta T)/T$.

Simulating according to this bias will asymptotically lead to the following distribution of potential energy, assuming normality of the potential energy probability distribution²²:

$$P(U)^{1/\gamma} \propto e^{(U - \langle U \rangle)^2 / 2\gamma \Delta U^2}, \quad (3)$$

where $\langle U \rangle$ and ΔU^2 are the expected value and variance of the potential energy of the unbiased canonical sampling. This expression shows that under the WTE bias, the average energies are the same but the variance of distribution is increased by $\sqrt{\gamma}$. A bias factor of 1 thus leads to canonical sampling. Increasing the bias factor increases the fluctuations in potential energy.

EDS modifies the potential energy of a system with a maximum entropy linear bias in a collective variable.⁹ After equilibration, EDS will have the following biased potential energy:

$$U'(\mathbf{R}) = U(\mathbf{R}) + \alpha f(\mathbf{R}), \quad (4)$$

where α is a Lagrange multiplier determined from an equilibration process described in White *et al.*¹⁰ and $f(\mathbf{R})$ is a differentiable collective variable. α is selected such that $\langle f \rangle = \hat{f}$, where \hat{f} is a pre-determined value for what the expected value of the collective variable should be. In this work, we have experimentally determined NMR chemical shifts for \hat{f} . The limitation of EDS is that finding α requires calculating $\langle f \rangle$ with good sampling of the underlying canonical distribution. The PT-WTE method can ensure we have sufficient sampling of the distribution of f values. The WTE process only needs to be modified to replace $U(\mathbf{R})$ with $U'(\mathbf{R})$ and the previous analysis holds.

The benefit of WTE is that the increased energy fluctuations arising from the choice of bias factor can improve replica-exchange efficiency in a parallel-tempering setting. The probability of exchange for replicas i and j becomes³⁴

$$P(\text{ex } i, j) = \min[1, \exp(\gamma^{-1} \beta_i [U'_i(\mathbf{R}_i) - U'_i(\mathbf{R}_j)] + \gamma^{-1} \beta_j [U'_j(\mathbf{R}_j) - U'_j(\mathbf{R}_i)])], \quad (5)$$

where $\beta_i = 1/k_B T_i$ and U'_i is the potential energy of the i th replica including the EDS bias. Note that EDS will have different α for each replica because $\langle f \rangle$ is a function of temperature. This exchange rule ensures that the resulting simulation will arrive at a canonical distribution without re-weighting. The result of this method is both an enhanced-sampled ensemble and a value for α .

3. Methods

A short peptide GYG was simulated with EDS¹⁰ and PT-WTE²² to enhance sampling and improve fit to experimental NMR chemical shifts from Platzer *et al.*³⁰ To compare the performance of EDS with enhanced sampling to other simulations, EDS with PT-WTE was compared to a single replica-unbiased simulation, a single replica-biased simulation, a parallel-tempering replica-exchange molecular dynamics (PT) simulation, and replica-unbiased PT-WTE simulation.

About 0.008 mg/cm³ of GYG peptide in 10 mM NaCl counter-ions was first energy minimized, then annealed and equilibrated in the NVT ensemble using the Canonical Sampling through Velocity Rescaling (CSVR) thermostat.³⁵ The CHARMM27³⁶ force field and TIP3P³⁷ water model were used throughout. Electrostatic forces were calculated with the particle mesh Ewald method³⁸, and dispersion forces were calculated with shifted van der Waals potentials with a cutoff distance of 10 Å. The covalent hydrogen bonds were constrained using the LINCS algorithm³⁹ to enable a 2 fs time step. All simulations were performed in the Gromacs-5.1.4 simulation engine.⁴⁰ To automatically run Gromacs commands in python, Gromacs-Wrapper was used.⁴¹ To generate an initial extended structure of GYG, the python package PeptideBuilder was used.⁴²

An equilibration is required for the PT-WTE method. Sixteen replicas of PT-WTE were tuned for 400 ps to find parameters that gave increased replica efficiency. The replica temperatures used for the 16 replica systems were 293, 299, 304, 310, 316, 323, 329, 336, 342, 349, 355, 363, 370, 377, 385, and 392 K, as generated by the method of Nemoto *et al.*⁴³ The exchanges were attempted every 250 time steps. The WTE parameters were chosen following Barducci *et al.*³³ and are shown in Table 1.

After the aforementioned short PT-WTE equilibration step, EDS was begun with the static bias from PT-WTE equilibration step. This combined PT-WTE with EDS had 16 replicas with the same set of temperatures as mentioned above and was 40 ns long. To control against the presence of either EDS bias, or PT-WTE bias, or both biases, 16 replicas of 40 ns PT simulations with and without EDS bias in the absence of WTE bias and 16 replicas of 40 ns PT-WTE simulations with and without EDS bias were run and are shown in Table 1. The large amount of time is not necessary for the convergence of EDS, but was chosen to get good sampling statistics. The EDS collective variables biased were chemical shifts³⁰ calculated via the Plumed2 molecular simulation plugin⁴⁴. The EDS parameters chosen are shown in Table 1.

Eight replicas of PT-WTE simulation were also done with and without EDS. These simulations demonstrate how PT-WTE can use fewer replicas than PT and still achieve good efficiency. The parameters are in Table 1. The replicas ran at the following temperatures: 293, 306, 320, 335, 350, 366, 383, and 400 K. Similar to 16 replicas of PT-WTE, 8 replicas of PT-WTE initially consisted of 400 ps equilibration step, followed by a static production step of 40 ns. There were 3620 atoms in

Table 1. Overview of simulation systems and their parameters.

Simulation parameters	EDS + PT-WTE ^a	No EDS + PT-WTE ^a	EDS + PT	No EDS + PT	Exp ^b
Replicas	16	16	16	16	—
Bias factor	10	10	—	—	—
Hill width (kJ/mol)	100	100	—	—	—
Hill height (kJ/mol)	0.1	0.1	—	—	—
Dim. Prop	0.2	—	0.2	—	—
Range	0.01	—	0.01	—	—
Time (ns)	40(0.4) ^a	40(0.4) ^a	40	40	—
Results					
C β δ (ppm)	38.52 \pm 2.35	36.39 \pm 2.13	38.48 \pm 1.84	39.06 \pm 2.89	38.60 \pm 0.08
C α δ (ppm)	57.89 \pm 3.21	59.38 \pm 2.35	57.93 \pm 3.25	58.23 \pm 3.34	58.00 \pm 0.08
H δ (ppm)	8.29 \pm 0.50	8.20 \pm 0.48	8.20 \pm 0.46	8.25 \pm 0.47	8.16 \pm 0.02
H α δ (ppm)	4.58 \pm 0.51	4.04 \pm 0.52	4.54 \pm 0.42	4.61 \pm 0.55	4.55 \pm 0.02
CO δ (ppm)	176.28 \pm 1.30	174.78 \pm 1.11	176.25 \pm 1.26	175.34 \pm 1.64	176.30 \pm 0.08
N δ (ppm)	120.06 \pm 5.34	118.34 \pm 7.43	120.09 \pm 5.35	119.88 \pm 6.58	120.1 \pm 0.08
Repl Efficiency (%)	39(31) ^a	21(31) ^a	22	23	—
Aver Efficiency (%)	41(40) ^a	28.2(40) ^a	23	25	—
Simulation parameters	EDS + PT-WTE	No EDS + PT-WTE	EDS + No PT	No EDS + No PT	Exp ^b
Replicas	8	8	1	1	—
Bias factor	20	20	—	—	—
Hill width (kJ/mol)	250	250	—	—	—
Hill height (kJ/mol)	1	1	—	—	—
Dim. Prop	0.2	—	0.2	—	—
Range	0.001	—	0.01	—	—
Time (ns)	40(0.4) ^a	40(0.4) ^a	40	40	—
Results					
C β δ (ppm)	38.48 \pm 2.06	37.77 \pm 3.05	38.47 \pm 1.71	39.18 \pm 2.58	38.60 \pm 0.08
C α δ (ppm)	57.94 \pm 3.35	58.91 \pm 3.14	57.94 \pm 3.06	57.99 \pm 3.33	58.00 \pm 0.08
H δ (ppm)	8.20 \pm 0.47	8.22 \pm 0.48	8.37 \pm 0.50	8.21 \pm 0.49	8.16 \pm 0.02
H α δ (ppm)	4.54 \pm 0.45	4.26 \pm 0.61	4.54 \pm 0.41	4.68 \pm 0.51	4.55 \pm 0.02
CO δ (ppm)	176.25 \pm 1.30	175.00 \pm 1.55	176.30 \pm 1.14	175.40 \pm 1.54	176.30 \pm 0.08
N δ (ppm)	120.12 \pm 5.49	117.90 \pm 7.20	120.01 \pm 4.79	119.43 \pm 5.84	120.1 \pm 0.08
Repl Efficiency (%)	55 (40) ^a	43(39) ^a	—	—	—
Aver Efficiency (%)	62 (51) ^a	58(53) ^a	—	—	—

Notes: These are the computed averages during various simulations. Both 2.5th and 97.5th percentile of the computed values are shown as well. The EDS and PT-WTE parameters are shown first as well as the simulation time. The chemical shifts are the cumulative averages. The replica-exchange efficiency is the percentage of attempted replica swaps that are successful for the least efficient replica. The average is the efficiency averaged over all replicas.

(a) PT-WTE was equilibrated for 400 ps and then restarted without further addition of gaussian hills for the 40 ns simulation. RMSD due to Camshift⁴⁵ for N,HN,HA,CA,CB, and C are 3.01,0.56,0.28,1.3,1.36, and 1.38 ppm.

(b) Experimental values are from Platzer *et al.*³⁰

the simulation with 1197 TIP3P water molecules and 38 peptide atoms. We used bias factor of 10 for 16 replicas of PT-WTE and 20 for 8 replicas of PT-WTE. Deighen *et al.* studied the effect of bias factor in 10 replicas of simulation that studied 39 amino acids long Trp-cage protein.²³ They found that increasing the bias factor from 10 to 24 decreased the time it takes to converge to the reference FES.²³ Hence, we used larger bias factor for 16 replicas of PT-WTE compared to 8 replicas of PT-WTE.

4. Results and Discussion

Table 1 provides an overview of the simulations run for this work. Multiple combinations of enhanced sampling methods with and without EDS were simulated. Each simulation ran for 40 ns. Sixteen replicas of PT-WTE simulations were equilibrated for 400 ps to find the biasing potentials that increased the replica-exchange efficiency, prior to enabling EDS. This PT-WTE tune step was run long enough to ensure that the efficiency exceeded 30%. Parallel-tempering replica-exchange (PT) with 16 replicas has 23% replica efficiency, as shown in Table 1. The replica efficiency is defined here as the minimum acceptance rate of configuration swapping between replicas. In other words, the lowest among the 16 replicas is taken to be the efficiency. This ensures that all replicas exchange at certain threshold rate prohibiting a different independent system of simulations that are exchanging only with replicas that have closer temperatures. The averages are also shown for the 40 ns simulations. Replica-exchange of 20% is the minimum for a well-sampled system,⁴⁰ and thus 16 was the minimum number of replicas for PT.

The choice of PT-WTE simulation parameters achieved good exchange with the smaller, 8 replicas system, despite spanning the same temperature range as the 16 replicas systems (293 K–400 K). Since 8 replicas system had a different set of WTE parameters, EDS parameters were modified as well, which included the reduction of the speed of convergence of EDS (lower range parameter) and increased the speed of convergence of the PT-WTE method (larger hill height).²² The bias factor was correspondingly decreased to reduce the strength of bias more quickly. PT-WTE with 16 replicas had smaller replica efficiency than 8 replicas PT-WTE in Table 1. This may be the result of a different set WTE and EDS parameters used in 8 replicas and 16 replicas simulations.

The EDS method moved the calculated backbone chemical shifts to the experimental values when applied as seen in Table 1. There is a good agreement between the average chemical shifts in the EDS simulations and experiments with any of the enhanced sampling methods applied. Even with the slower parameters used in the 8 replica system, the EDS method still achieved the correct values.

Figure 1 shows the cumulative calculated mean backbone chemical shifts over time during 16 replica PT-WTE with EDS bias, (a) 16 replicas of PT-WTE without EDS, (b) 16 replicas of PT with EDS, (c) 16 replicas of PT without EDS, 8 replicas of PT-WTE with EDS (e), 8 replicas of PT-WTE without EDS (f), single replica of EDS (g), and a standard MD (h). Chemical shifts were modified to show the absolute difference between cumulative averages and the corresponding experimental chemical shifts. Therefore, the exact match between simulation and experiment is indicated by the convergence of cumulative calculated mean chemical shifts to 0. As expected, EDS-biased average chemical shifts converge to the reference value with 16 replicas of PT-WTE (Fig. 1(a)), with 16 replicas of PT (Fig. 1(c)), and with 8 replicas of PT-WTE (Fig. 1(e)). EDS does not make instantaneous values of biased chemical shifts which converge with the reference value, but makes the ensemble

average to approach the reference value as shown in Fig. S1 of the Supporting Information. In all of the EDS cases (Figs. 1(a), 1(c), 1(e), and 1(g)), EDS converges within 1 ns. In all EDS bias simulations (Figs. 1(a), 1(c), 1(e), and 1(g)), average chemical shifts of the hydrogen connected to backbone nitrogen atom had the highest

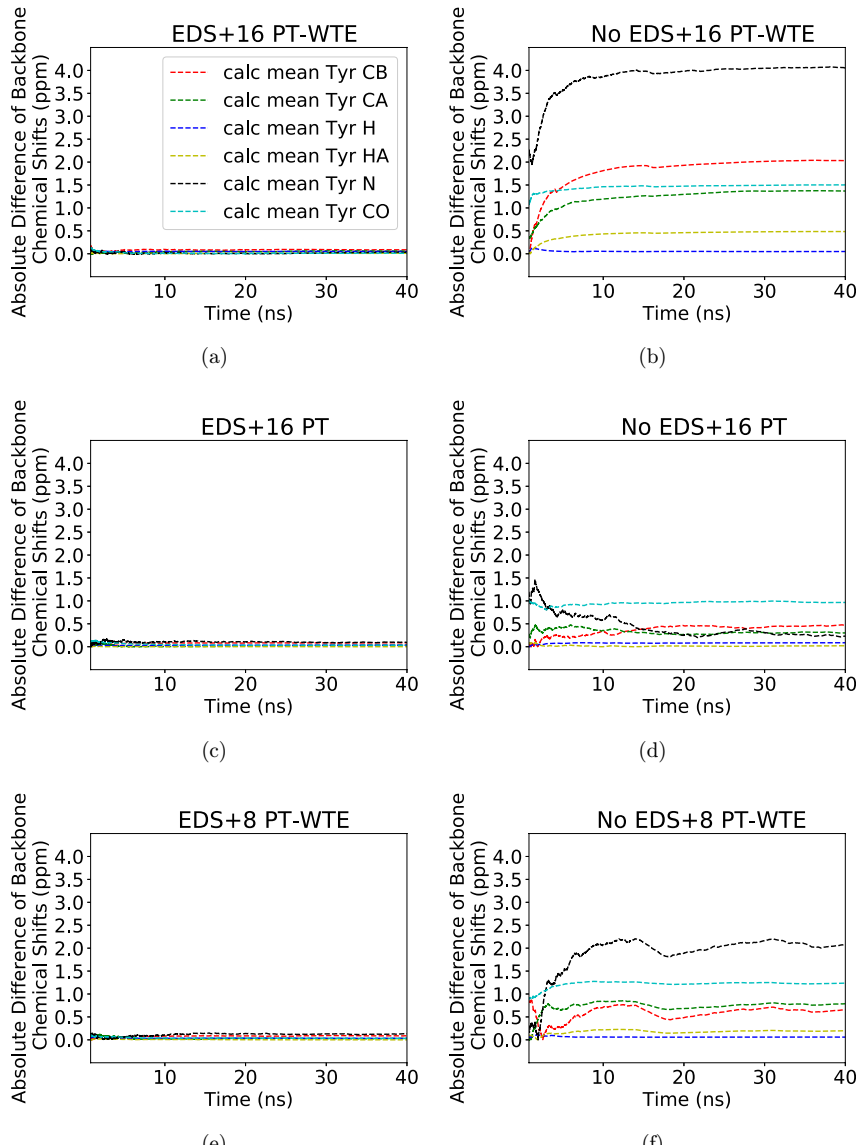


Fig. 1. Convergence of chemical shifts to the reference experimental value. Absolute difference between calculated cumulative average and experimental chemical shifts are shown. EDS was used with PT-WTE for enhanced sampling as shown in (a). (b) Shows that without EDS. (c) EDS with 16 replicas of PT converges to experiments. The lack of EDS lowers the convergence (d). (e) Displays with fewer replicas, EDS still converges to experiments. (f) Without EDS, agreement with experiments is poor.

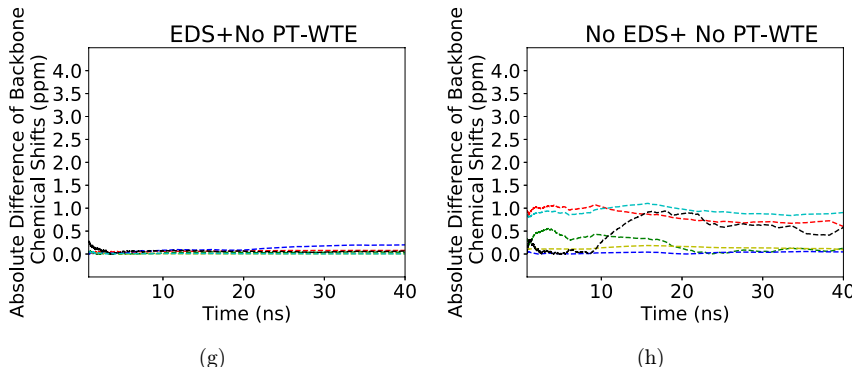


Fig. 1. (Continued)

deviation from the predicted value when compared to other atoms. The Camshift root mean square deviation for H connected to N is 0.56 ppm, whereas Camshift predicts deviations to be the highest for N with RMSD of 3.01 ppm in a 28 protein test set.⁴⁵ During 40 ns simulation, the cumulative average backbone ¹⁵N chemical shift was within 1% of the reference chemical shift. Since PT-WTE and PT swap configurations between different temperature replicas, chemical shifts also change whenever the conformations change as indicated by the greater fluctuations between mean chemical shifts and reference values in PT-WTE and PT with EDS (Figs. 1(a), 1(c) and 1(d)) simulation compared to single replica EDS (Fig. 1(g)). In the absence of EDS bias, average chemical shifts in various simulations, shown in Figs. 1(b)–1(f), do not converge to 0 because the simulation is less accurate. When EDS was absent in both 16 replicas of PT-WTE (Fig. 1(b)) and 16 replicas of PT (Fig. 1(d)), the average chemical shifts fluctuated more drastically in Fig. 1(b) compared to simulation without PT-WTE as shown in Fig. 1(d). This is due to the better exploration of phase-space with the PT-WTE method. The convergence under a variety of enhanced sampling methods shows that EDS still works well when combined with enhanced sampling.

To see the effect of enhanced sampling and the effect of biased chemical shifts to other collective variables in a simulation, Φ and Ψ dihedral angles were compared to regular unbiased MD and to Ramachandran plots from X-ray crystallography.⁴⁶ The simulated free energy landscapes of Tyrosine in GYG peptide along Φ and Ψ dihedral angles are displayed in Fig. 2. Dihedral angles were computed during the simulations and their histograms were used to compute the FES. EDS predicted the same global minimum regardless of presence (Fig. 2(a)) or absence of PT-WTE (Fig. 2(c)) at $\Phi = -1.2$ and $\Psi = -0.9$. The free energy surface shows different global minimum with EDS because the free energy distribution is biased to satisfy experimental conditions. As shown in Figs. 2(a) and 2(c), EDS simulations show the global minimum to be at $\Phi = -1.2$ and $\Psi = -0.9$, different from the one observed by enhanced

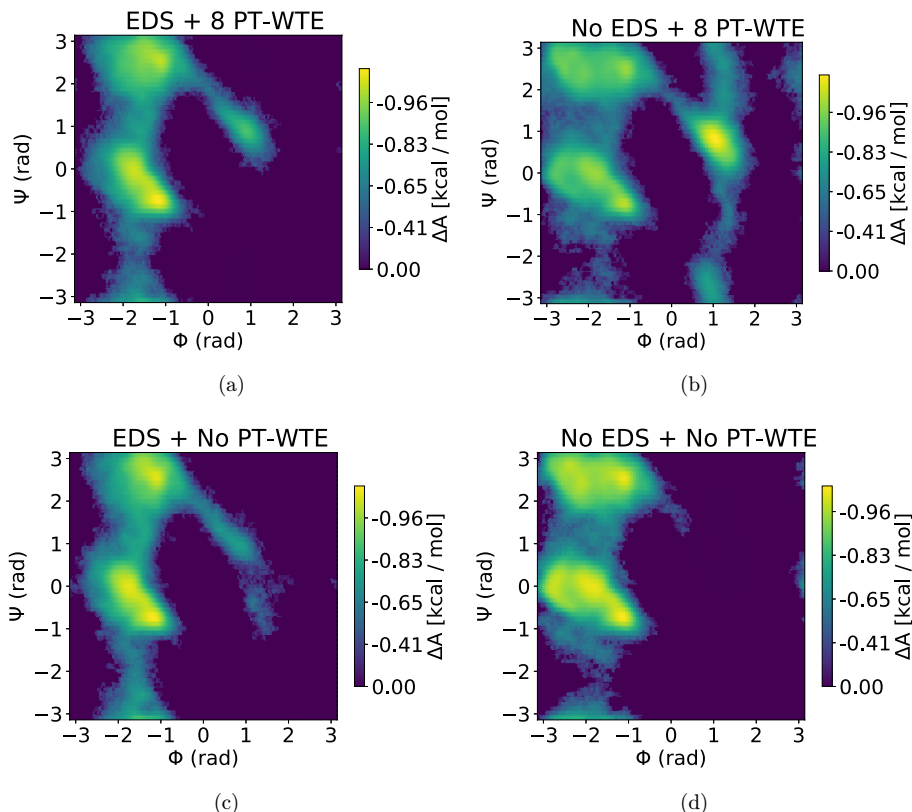


Fig. 2. Free energy surface (FES) of Φ - Ψ dihedral angles of Y amino acid from GYG simulations. (a) shows the FES with EDS and PT-WTE so that backbone chemical shifts match experimental values and sampling is enhanced. (b) without EDS bias, PT-WTE explores Φ around 1.5 and Ψ in $[-3.14, 3.14]$ interval more, and finds a global minimum at about $\Phi = 1.5$ and $\Psi = 1$. (c) shows less sampling of global minimum at $\Phi = 1.5$ radians and $\Psi = 1$, compared to (a). (d) shows no exploration of the global minimum at $\Phi = 1.5$ and $\Psi = 1$ and seems to be stuck on negative Φ angles. All FESs were generated from a 20 ns NVT simulation at 293 K.

sampling alone (Fig. 2(b)). PT-WTE (Fig. 2(b)) found a different global minimum at around $\Phi = 1.2$ and $\Psi = 1$ in the absence of EDS compared to the presence of EDS (Fig. 2(a)). Also, PT-WTE without EDS explored a region at $\Phi = 1$ and Ψ in the $[-\pi, \pi]$ in Fig. 2(b). This is similar to Tyrosine Ramachandran plot from Vitalini *et al.*⁴⁷ and from Ting *et al.*⁴⁶ neither of the single replica EDS (Fig. 2(c)), EDS with PT-WTE (Fig. 2(a)) nor regular MD (Fig. 2(d)) sampled this region. Although EDS in the presence of PT-WTE (Fig. 2(a)) did not show aberrant behavior from the absence of PT-WTE in Fig. 2(c), it showed improved sampling of global minimum observed in PT-WTE alone at Φ around 1 radians and at $\Psi = 1$ radians compared to the absence of PT-WTE (Fig. 2(c)) and regular MD (Fig. 2(d)). Overall, PT-WTE improved sampling and EDS modified the FES to achieve agreement with the NMR chemical shifts.

Ramachandran plots from Ting *et al.*⁴⁶ of Tyrosine in the sequence GYG were compared to our results. The result of Ting *et al.*⁴⁶ are derived from a bioinformatics analysis of X-ray crystallographic data of whole proteins. Tyrosine dihedral angle plot of Tyrosine in YG peptide from Ting *et al.*⁴⁶ was compared to our results, since YG was closest to GYG. Ting *et al.* observed three regions of minimum in Tyrosine: at about ($\Phi = -1.0$, $\Psi = 2.8$, which was the global minimum), ($\Phi = -1.0$, $\Psi = [-1, 1]$), and ($\Phi = 1$, $\Psi = 1$). Out of all the FES for simulations that are shown, Fig. 2(a) was closest to experimentally observed FES by Ting *et al.*,⁴⁶ because, local minimum at ($\Phi = 1$, $\Psi = 1$) was predicted correctly and minima at ($\Phi = -1.0$, $\Psi = 2.8$) and ($\Phi = -1.0$, $\Psi = [-1, 1]$) were close relative to each other in Ting *et al.*⁴⁶ and in Fig. 2(a). Ting *et al.*⁴⁶ also reported the global minima to be on the negative Φ angle axis. A local minimum at around $\Phi = 1$ and $\Psi = 1$ radians reported by Ting *et al.*,⁴⁶ was also observed as a minimum in Figs. 2(a)–2(c). This local minimum was not predicted by the standard MD at all within 20 ns, as seen in Fig. 2(d). EDS did not show drastic deviation in unbiased structural properties, such as a dihedral angle of Tyrosine. Indeed, dihedral angles in EDS simulations with or without enhanced sampling showed similar results as X-ray crystallography did.

Another major question about disagreement between simulations and experiments is whether the underlying cause is lack of sampling or inaccuracy of the force-field/system. Eight replicas of PT-WTE without EDS show that even with good sampling, the simulation matches neither the chemical shifts nor the FES from the EDS simulation, as shown in Fig. 2(b). This is not necessarily due to a deficiency in the CHARMM force field, but instead could be due to a difference in concentration, ions, and termini between the simulations and the work of Platzer *et al.*,³⁰ from which the chemical shifts were measured.

5. Conclusion

Simultaneous enhanced sampling and EDS was demonstrated on the GYG peptide in explicit solvent. EDS improved the accuracy of the simulation by minimally biasing the backbone chemical shifts of the peptide to match experimental data from Platzer *et al.*³⁰ Single replica simulations with and without EDS bias ran for comparable time. Both parallel-tempering replica-exchange (PT) and parallel-tempering well-tempered ensemble (PT-WTE) were used with EDS to improve sampling. Theory was presented to justify why using both concurrently preserves canonical sampling. Compared to the absence of enhanced sampling in normal MD, the system benefited from enhanced sampling. PT and PT-WTE provided improved sampling and did not interfere with EDS, with EDS converging within 1 ns. PT-WTE with 8 replicas spanning 293 K to 400 K was also demonstrated with EDS, showing that the PT-WTE method is able to reduce the number of replicas required relative to PT. We hope to use this new method on larger system to take advantage of both enhanced sampling and biasing with experiments.

Acknowledgments

Support for DB Amirkulova was provided by a Hopeman scholarship from the University of Rochester. Thanks to Rainier Barret for feedback and discussion of the paper. We are grateful for resources and services provided by Center for Integrated Research Computing at University of Rochester.

References

1. Bonomi M, Heller GT, Camilloni C, Vendruscolo M, Principles of protein structural ensemble determination, *Curr Opin Struct Biol* **42**:106–116, 2017. doi: 10.1016/j.sbi.2016.12.004.
2. Allison JR, Using simulation to interpret experimental data in terms of protein conformational ensembles, *Curr Opin Struct Biol* **43**:79–87, 2017. doi: 10.1016/j.sbi.2016.11.018.
3. Cavalli A, Salvatella X, Dobson CM, Vendruscolo M, Protein structure determination from NMR chemical shifts, *Proc Natl Acad Sci USA* **104**(23):9615–9620, 2007. 0610313104 [pii]10.1073/pnas.0610313104.
4. Robustelli P, Kohlhoff K, Cavalli A, Vendruscolo M, Using NMR chemical shifts as structural restraints in molecular dynamics simulations of proteins, *Structure* **18**(8):923–933, 2010. doi: 10.1016/j.str.2010.04.016.
5. Torda AE, Scheek RM, van Gunsteren WF, Time-averaged nuclear overhauser effect distance restraints applied to tendimistat, *J Mol Biol* **214**:223–235, 1990.
6. Jaynes E, Information theory and statistical mechanics, *Phys Rev A* **106**(4):620–621, 1957.
7. Boomsma W, Ferkinghoff-Borg J, Lindorff-larsen K, Combining experiments and simulations using the maximum entropy principle, *PLOS Comput Biol* **10**(2):1–9, 2014. doi: 10.1371/journal.pcbi.1003406.
8. Roux B, Weare J, On the statistical equivalence of restrained-ensemble simulations with the maximum entropy method, *J Chem Phys* **138**(8), 2013. doi: 10.1063/1.4792208.
9. Pitera JW, Chodera JD, On the use of experimental observations to bias simulated ensembles, *J Chem Theory Comput* **8**(10):3445–3451, 2012. doi: 10.1021/ct300112v.
10. White AD, Voth GA, Efficient and minimal method to bias molecular simulations with experimental data, *J Chem Theory Comput* **10**(8):3023–3030, 2014.
11. White AD, Dama JF, Voth GA, Designing free energy surfaces that match experimental data with metadynamics, *J Chem Theory Comput* **11**(6):2451–2460, 2015. doi: 10.1021/acs.jctc.5b00178.
12. Roux, B, Islam S, Restrained-ensemble molecular dynamics simulations based on distance histograms from double electron-electron resonance spectroscopy, *J Phys Chem B* **17**(117):4733–4739, 2013. doi: 10.1016/j.jacc.2007.01.076.White.
13. White AD, Knight C, Hocky GM, Voth GA, Communication: Improved ab initio molecular dynamics by minimally biasing with experimental data, *J Chem Phys* **146**(4):041102, 2017. doi: 10.1063/1.4974837.
14. Dannenhoffer-Lafage T, White AD, Voth GA, A Direct method for incorporating experimental data into multiscale coarse-grained Models, *J Chem Theory Comput.* **12**(5):2144–2153, 2016. doi: 10.1021/acs.jctc.6b00043.
15. Bonomi M, Camilloni C, Cavalli A, Vendruscolo M, Metainference: A Bayesian inference method for heterogeneous systems, *Sci. Adv.* **2**(1):e1501177, 2016. doi: 10.1126/sciadv.1501177.
16. Clarage JB, Romo T, Andrews BK, Pettitt BM, Phillips GN, A sampling problem in molecular dynamics simulations of macromolecules, *Proc Natl Acad Sci USA* **92**(8):3288–3292, 1995. doi: 10.1073/pnas.92.8.3288.

17. Bernardi RC, Melo MC, Schulten K, Enhanced sampling techniques in molecular dynamics simulations of biological systems, *Biochim et Biophys Acta (BBA) — General Subjects* **1850**(5):872–877, 2015. doi: 10.1016/j.bbagen.2014.10.019.
18. Darve E, Rodriguez-Gomez D, Pohorille A, Adaptive biasing force method for scalar and vector free energy calculations, *J Chem Phys* **128**(14):1–13, 2008. doi: 10.1063/1.2829861.
19. Laio A, Parrinello M, Escaping free-energy minima, *Proc Natl Acad Sci USA* **99**(20):12562–12566, 2002. doi: 10.1073/pnas.202427399.
20. Hansmann UHE, Parallel tempering algorithm for conformational studies of biological molecules, *Chem Phys Lett* **281**(or L):140–150, 1997.
21. Bittner E, Nubaumer A, Janke W, Make life simple: Unleash the full power of the parallel tempering algorithm, *Phys Rev Lett* **101**(13):1–4, 2008. doi: 10.1103/PhysRevLett.101.130603.
22. Bonomi M, Parrinello M, Enhanced sampling in the well-tempered ensemble, *Phys Rev Lett* **104**(19):1–4, 2010. doi: 10.1103/PhysRevLett.104.190601.
23. Deighan M, Bonomi M, Pfaendtner J, Efficient simulation of explicitly solvated proteins in the well-tempered ensemble, *J Chem Theory Comput* **8**(7):2189–2192, 2012. doi: 10.1021/ct300297t.
24. Spiwok V, Sucur Z, Hosek P, Enhanced sampling techniques in biomolecular simulations, *Biotechnol Adv* **33**(6):1130–1140, 2015. doi: 10.1016/j.biotechadv.2014.11.011.
25. Bella J, Liu J, Kramer R, Brodsky B, Berman HM, Conformational effects of Gly – X – Gly interruptions in the collagen triple helix, *J Mol Biol* **362**:298–311, 2006. doi: 10.1016/j.jmb.2006.07.014.
26. Dibb KM, Rose T, Makary SY, Claydon TW, Enkvetchakul D, Leach R, Nichols CG, Boyett MR, Molecular basis of ion selectivity, block, and rectification of the inward rectifier Kir3. 1/Kir3. 4 K channel, *J Biol Chem* **278**(49):49537–49548, 2003. doi: 10.1074/jbc.M307723200.
27. Thiagarajan G, Li Y, Mohs A, Strafaci C, Popiel M, Baum J, Brodsky B, Common interruptions in the repeating tripeptide sequence of non-fibrillar collagens: Sequence analysis and structural studies on triple-helix peptide models, *J Mol Biol* **376**:736–748, 2008. doi: 10.1016/j.jmb.2007.11.075.
28. So I, Ashmole I, Davies NW, Sutcliffe MJ, Stanfield PR, The K + channel signature sequence of murine Kir2.1: mutations that affect microscopic gating but not ionic selectivity, *J Physiol* **531**(1):37–50, 2001.
29. Bernèche S, Roux B, A gate in the selectivity filter of potassium channels, *Structure* **13**:591–600, 2005. doi: 10.1016/j.str.2004.12.019.
30. Platzer G, Okon M, McIntosh LP, pH-dependent random coil 1 H, 13 C, and 15 N chemical shifts of the ionizable amino acids: A guide for protein p K a measurements, *J Biomol NMR* **60**(2–3):109–129, 2014. doi: 10.1007/s10858-014-9862-y.
31. Bonomi M, Camilloni C, Vendruscolo M, Metadynamic metainference: Enhanced sampling of the metainference ensemble using metadynamics, *Sci Rep* **6**(July):1–11, 2016. doi: 10.1038/srep31232.
32. Camilloni C, Cavalli A, Vendruscolo M, Replica-averaged metadynamics, *J Chem Theory Comput* **9**(12):5610–5617, 2013. doi: 10.1021/ct4006272.
33. Barducci A, Bussi G, Parrinello M, Well-tempered metadynamics: A smoothly converging and tunable free-energy method, *Phys Rev Lett* **100**(2):1–4, 2008. doi: 10.1103/PhysRevLett.100.020603.
34. Bussi G, Hamiltonian replica exchange in GROMACS: A flexible implementation, *Mol Phys* **112**(3–4):379–384, 2014. doi: 10.1080/00268976.2013.824126.
35. Bussi G, Donadio D, Parrinello M, Canonical sampling through velocity rescaling, *J Chem Phys* **126**(1):014101, 2007. doi: 10.1063/1.2408420.

36. Pastor RW, MacKerell AD Jr, Development of the CHARMM force field for lipids, *J Phys Chem Lett* **2**(13):1526–1532, 2011. doi: 10.1021/jz200167q.
37. Jorgensen WL, Chandrasekhar J, Madura JD, Impey RW, Klein ML, Comparison of simple potential functions for simulating liquid water, *J Chem Phys* **79**(2):926–935, 1983. doi: 10.1063/1.445869.
38. Essmann U, Perera L, Berkowitz ML, Darden T, Lee H, Pedersen LG, A smooth particle mesh Ewald method A smooth particle mesh Ewald method, *J Chem Phys* **103**(19):8577–8593, 1995. doi: 10.1063/1.470117.
39. Hess B, Bekker H, Berendsen HJC, Fraaije JGEM, LINCS: A linear constraint solver for molecular simulations, *J Comput Chem* **18**(12):1463–1472, 1997. doi: 10.1002/(SICI)1096-987X(199709)18:12<1463::AID-JCC4>3.0.CO;2-H.
40. James M, Murtola T, Schulz R, Smith JC, Hess B, Lindahl E, ScienceDirect GROMACS: High performance molecular simulations through multi-level parallelism from laptops to supercomputers, *SoftwareX* **2**:19–25, 2015. doi: 10.1016/j.softx.2015.06.001.
41. Beckstein O *et al.*, GromacsWrapper, <https://github.com/Becksteinlab/GromacsWrapper>, doi: 10.5281/zenodo.17901.
42. Tien MZ, Sydykova DK, Meyer AG, Wilke CO, Peptide builder: A simple Python library to generate model peptides, Paci E (ed.) *PeerJ* **1**:e80, 2013. doi:10.7717/peerj.80.
43. Hukushima K, Nemoto K, Exchange monte carlo method and application to spin glass simulations, *J Phys Soc Jpn* **65**(6):1604–1608, 1995.
44. Tribello GA, Bonomi M, Branduardi D, Camilloni C, Bussi G, PLUMED 2: New feathers for an old bird, *Comput Phys Commun* **185**(2):604–613, 2014. doi: 10.1016/j.cpc.2013.09.018.
45. Kohlhoff KJ, Robustelli P, Cavalli A, Salvatella X, Vendruscolo M, Fast and accurate predictions of protein NMR chemical shifts from interatomic distances, *J Am Chem Soc* **131**(39):13894–13895, 2009. doi: 10.1021/ja903772t.
46. Ting D, Wang G, Shapovalov M, Mitra R, Jordan MI, Dunbrack RL, Neighbor-dependent Ramachandran probability distributions of amino acids developed from a hierarchical dirichlet process model, *PLoS Comput Biol* **6**(4), 2010. doi: 10.1371/journal.pcbi.1000763.
47. Vitalini F, Noé F, Keller B, Molecular dynamics simulations data of the twenty encoded amino acids in different force fields, *Data Brief* **7**:582–590, 2016. doi: 10.1016/j.dib.2016.02.086.